Energy Relaxation in the Integer Quantum Hall Regime

H. le Sueur, C. Altimiras, U. Gennser, A. Cavanna, D. Mailly, and F. Pierre*

CNRS, Laboratoire de Photonique et de Nanostructures (LPN)—Phynano team, route de Nozay, 91460 Marcoussis, France

(Received 22 March 2010; published 27 July 2010)

We investigate the energy exchanges along an electronic quantum channel realized in the integer quantum Hall regime at a filling factor of $\nu_L = 2$. One of the two edge channels is driven out of equilibrium and the resulting electronic energy distribution is measured in the outer channel, after several propagation lengths $0.8\ \mu\text{m} \leq L \leq 30\ \mu\text{m}$. Whereas there are no discernible energy transfers toward thermalized states, we find efficient energy redistribution between the two channels without particle exchanges. At long distances $L \geq 10\ \mu$m, the measured energy distribution is a hot Fermi function whose temperature is lower than expected for two interacting channels, which suggests the contribution of extra degrees of freedom. The observed short energy relaxation length challenges the usual description of quantum Hall excitations as quasiparticles localized in one edge channel.

DOI: 10.1103/PhysRevLett.105.056803 PACS numbers: 73.43.Fj, 72.15.Lh, 73.23.Ad, 73.43.Lp

The basic manifestation of the quantum Hall effect is a quantized Hall resistance $R_H = h/e^2\nu_L$, accompanied by a vanishing longitudinal resistance. In this regime, quantization of the two-dimensional cyclotron motion opens a large gap separating Landau levels in the bulk of the sample from the Fermi energy. The only available low energy excitations propagate along the edges, where the Landau levels cross the Fermi energy. The effective edge state theory suggests these excitations are prototypal one-dimensional chiral fermions (1DCF) [1], each of the ν_L edge channels (EC) being identified with a one-dimensional conductor. Because backscattering is forbidden by chirality, ECs are considered to be ideal ballistic quantum channels. Their similitude with light beams has inspired electronic analogues of quantum optics experiments [2–5] and proposals for quantum information applications [6]. However, the nature and decoherence of edge excitations are poorly understood, as highlighted by unexpected results obtained with electronic Mach-Zehnder interferometers: an unusual energy dependence of the interference fringes' visibility [2,7], a non-Gaussian noise [8], and a short coherence length [9,10]. Interactions between ECs and with their environment are seen as the key ingredient to explain these results (see, e.g., [11,12]).

In the present experimental work, we investigate the interaction mechanisms taking place along an EC through the energy exchanges they induce. A similar approach was previously used on mesoscopic metal wires [13] and on carbon nanotubes [14]. Here we focus on the filling factor $\nu_L = 2$, where two copropagating ECs are present, and at which the above unexpected results were observed. Our experiment relies on the techniques we recently demonstrated to drive out of equilibrium an EC and to measure the resulting energy distribution $f(E)$ of 1DCF quasiparticles [15]. There, we drove out of equilibrium only the outer EC, and $f(E)$ was measured in the same EC after a short 0.8 μm propagation distance, for which the energy redistribution is negligible. Here, we drive out of equilibrium selectively either the inner or the outer EC and probe $f(E)$ in the outer EC after various, much longer, propagation paths, up to 30 μm. The electronic energy transfers, including those within and between the ECs, are revealed through changes in $f(E)$ along the edge. This gives us access to the underlying interaction mechanisms.

The measured sample displayed in Fig. 1 was tailored in a two-dimensional electron gas realized in a GaAs/Ga(Al)As heterojunction of density 2×10^{15} m^{-2}, mobility $\mu = 250$ m^2 V^{-1} s^{-1}, and measured in a dilution refrigerator of base temperature 30 mK [16]. The relevant ECs are defined by voltage biased surface metallic gates

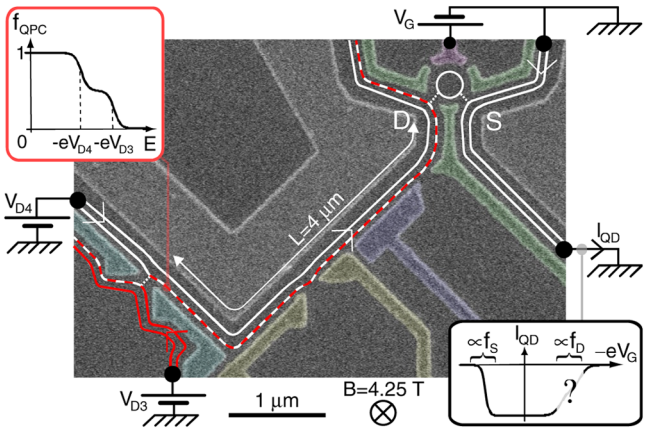

FIG. 1 (color online). Sample micrograph: metallic gates appear bright; the two widest gates (not colorized) are grounded. The current propagates counterclockwise along two edge channels (EC) depicted by lines. White dashed lines indicate intermediate EC transmissions. At the output of the voltage biased quantum point contact (left in figure), the electronic energy distribution is a double step (left inset) in the partly transmitted EC (dashed outer EC in figure). After an adjustable propagation distance ($L = 4$ μm in figure), the energy distribution f_D in the outer EC is measured using a quantum dot (white circle, see right inset).

(except a small portion defined by mesa etching for the longest propagation paths, see [16]). The energy distribution $f_D(E)$ in the outer EC at the drain (D) side of a quantum dot (QD, white circle in Fig. 1) is probed using the QD as an energy spectrometer, as has already been described in [15]: We record the differential conductance $\partial I_{\rm QD}(V_G)/\partial V_G \propto \partial f_D(E)/\partial E$, with $I_{\rm QD}$ the tunnel current across the small QD set to have a single active electronic level, while sweeping the voltage V_G applied to a capacitively coupled gate [15]. The path length $L \in \{0.8, 2.2, 4, 10, 30\}$ μm is tuned *in situ* by first choosing the pair of metallic gates that define the quantum point contact (QPC) at which a nonequilibrium energy distribution $f_{\rm QPC}$ is induced, and then by applying a negative voltage to selected gates to define the path between the QPC and the QD. A nonequilibrium smeared double step $f_{\rm QPC}(E)$ [15] is induced at the output of the voltage biased QPC selectively in the outer or inner EC by adjusting the QPC's conductance to $0.5e^2/h$ or $1.5e^2/h$, which are illustrated in Figs. 2(a) and 3(a), respectively.

First, we generate a nonequilibrium energy distribution in the measured *outer* EC [Fig. 2(a)]. The raw $\partial I_{\rm QD}/\partial V_G$ data are shown in Fig. 2(b) for several lengths L, at fixed QPC voltage bias $\delta V_D = 36$ μV. For the shortest propagation length $L = 0.8$ μm, we find a double dip close to expectations for noninteracting ECs and, consequently, that energy exchanges are small on this scale [15]. As L is increased the signal evolves toward a single dip. This demonstrates energy exchanges, which occur here on a characteristic length $L_{\rm inel} \approx 3$ μm [16]. At the two longest propagation paths, we find the *same* broad dip within experimental accuracy. It corresponds to a drain Fermi distribution of temperature $T_{\rm hot} = 85$ mK (solid lines on top of data at $L = 10$ and 30 μm), much larger than the equilibrium dip's temperature $T_{\rm eq} = 40$ mK (data at $\delta V_D = 0$ are shown for comparison as a dotted line). Complementary tests were performed to ascertain the observed energy exchanges are not artifacts [16].

We now investigate the interaction mechanisms responsible for the established energy exchanges. A simple mechanism could be the tunneling of charges between copropagating ECs, but we found it is here negligible [16]. In particular, anomalous quantum Hall effect measurements [17] showed that there is here no equilibration along the considered paths between the different electrochemical potentials of the two copropagating ECs. Important information to elucidate the interaction mechanisms can be obtained from the total energy $E_{\rm out}$ of the probed outer EC's 1DCFs. Let us consider several scenarios. (i) If interactions are essentially between 1DCFs in the same EC, then energy conservation in the stationary regime implies $E_{\rm out}$ is unchanged along the propagation path. On the other hand, (ii) if there is a significant interaction with thermalized states, such as the many quasiparticles within the surface metal gates along sample edges or the phonons, then $E_{\rm out}$ should relax toward its cold equilibrium

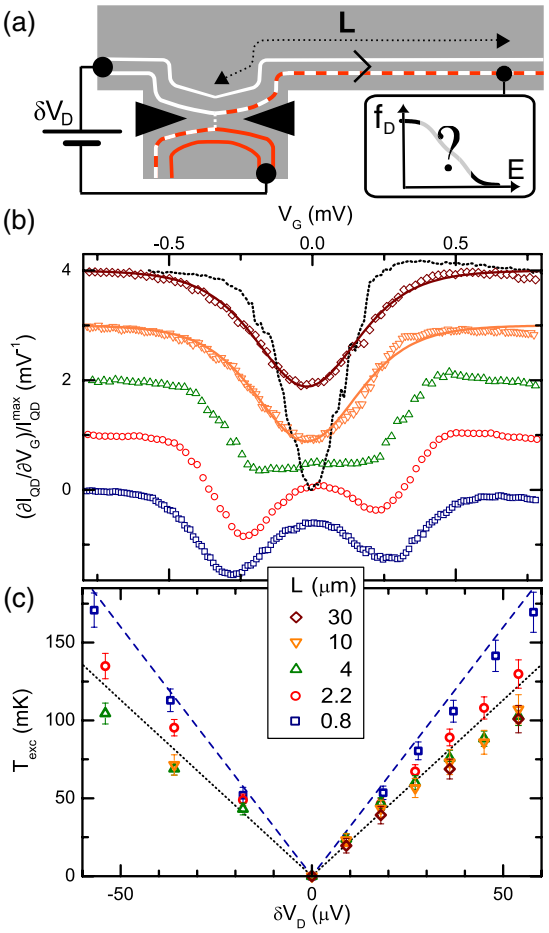

FIG. 2 (color online). (a) The outer EC is driven out of equilibrium. (b) Raw data (symbols) at $\delta V_D = 36$ μV, shifted vertically for several L. The nonequilibrium double dip relaxes over $L_{\rm inel} \approx 3$ μm toward a dip broader than the equilibrium dip at $\delta V_D = 0$ (dotted line). Solid lines are calculations with a Fermi distribution at 85 mK. (c) Excess temperatures extracted from the data (symbols) and prediction at the QPC output (dashed line). The outer EC cools down as L is increased and saturates at a value below expectations for two interacting ECs (dotted line, see text).

value $E_{\rm out}(\delta V_D = 0)$, or, if either the coupling constant or the density of these states vanishes at low energies, toward a fixed value at large δV_D. Last, (iii) if interactions are essentially with other copropagating states, then the injected energy redistributes. Therefore $E_{\rm out}$ should decrease to a value above $E_{\rm out}(\delta V_D = 0)$ by an amount proportional to the injected energy. The copropagating states could be the inner EC's 1DCFs or/and additional internal EC modes [18] that are predicted to exist in most situations due to edge reconstruction [19].

Figure 2(c) shows the outer EC's energy for various L and δV_D as the generalized excess temperature $T_{\rm exc} \equiv \sqrt{6[E_{\rm out} - E_{\rm out}(\delta V_D = 0)]/\nu\pi^2 k_B^2}$ (symbols), with ν the outer EC's density of states per unit length and energy. The ratio $E_{\rm out}/\nu$ can be obtained from f_D using

$$E_{\mathrm{out}}/\nu = \int (E-\mu)[f_D(E) - \theta(\mu - E)]dE, \quad (1)$$

with $\theta(E)$ the step function and μ the electrochemical potential (the full procedure to extract T_{exc} is detailed in [16]). We find T_{exc} relaxes as L increases, from a value very close to the QPC output prediction $T_{\mathrm{exc}}^{\mathrm{qpc}} = \sqrt{3}e|\delta V_D|/(2\pi k_B)$ (dashed line) at $L = 0.8$ μm, down to $T_{\mathrm{exc}} \approx (0.61 \pm 0.04)T_{\mathrm{exc}}^{\mathrm{qpc}}$ at $L = 10$ and 30 μm for $|\delta V_D| > 20$ μV. The saturation of T_{exc} at long propagation lengths to a value proportional to $T_{\mathrm{exc}}^{\mathrm{qpc}}$ at the QPC output is incompatible with significant dissipation toward thermalized states on the probed length scales [scenario (ii)]. Instead, this observation corresponds to expectations for interactions with copropagating states [scenario (iii)]. Last, energy exchanges between 1DCFs of the same EC [scenario (i)] are relatively weak compared to the dominant mechanism. Indeed, they preserve T_{exc}, whereas we find f_D and T_{exc} evolve on the same length scale, as seen in Figs. 2(b) and 2(c). Additional experiments not shown here further demonstrate that this energy exchange mechanism is negligible for $L \leq 10$ μm [20].

The data are compatible with energy redistribution with copropagating states, but which states? It is most natural to assume the 1DCFs of the two copropagating ECs exchange energy. This hypothesis can be tested directly by generating a nonequilibrium energy distribution in the inner EC ($G_{\mathrm{QPC}} \simeq 1.5e^2/h$), with f_D still being measured in the outer EC [see Fig. 3(a)]. Figure 3(b) shows raw data obtained in this configuration at $\delta V_D = 54$ μV for several L. We find that the dip broadens as L is increased, and therefore that the outer EC heats up. This unambiguously demonstrates energy exchanges between ECs. Figure 3(c) shows T_{exc} in the outer EC (symbols), which increases with L as expected from the raw data. Note that $T_{\mathrm{exc}}(L = 10$ μm) is approximately independent of which of the inner or the outer EC is driven out of equilibrium, as would be expected for a complete energy current equipartition between ECs.

These results are in qualitative agreement with recent investigations of dephasing at $\nu_L = 2$, which established current noise in one EC reduces phase coherence in the second EC [8,21]. The dephasing length $L_\phi(T) \simeq 20$ μm$/(T/20$ mK) [10] can be compared to the inelastic length. Using the injected excess temperature $T_{\mathrm{exc}}^{\mathrm{qpc}} = 115$ mK at $\delta V_D = 36$ μV, we find $L_\phi(115\ \mathrm{mK}) \simeq 3.5$ μm, similar to the corresponding $L_{\mathrm{inel}} = 2.5 \pm 0.4$ μm [16]. This strengthens the case for a same physical mechanism at the root of both dephasing and energy exchanges. However, contrary to dephasing [21], energy exchanges cannot be accounted for by low frequency noise within perturbation theories.

We now discuss different theoretical models aiming at explaining the present data. Within the widespread picture of 1DCF quasiparticles, the minimal approach is to include interactions between copropagating ECs as a small perturbation. However, in absence of disorder, energy exchanges between 1DCFs of different drift velocities v_D would be essentially suppressed, due to combined energy and momentum conservations. Therefore, it is crucial to assume a sufficient disorder to break momentum conservation. Motivated by the present work, Lunde *et al.* modeled inter EC interactions as a density-density coupling, where disorder changes the coupling coefficient along the edge with a correlation length ℓ [22]. Within this model, $T_{\mathrm{exc}}(L/L_0, \delta V_D)$ was obtained up to an unknown length scaling factor L_0. Comparing with the data, it was found that the nonlinear shape of $T_{\mathrm{exc}}(\delta V_D)$ can be reproduced using a reasonable micron-scale ℓ [22]. On the other hand, general arguments imply that two weakly interacting 1DCF branches cannot result in $T_{\mathrm{exc}} < T_{\mathrm{exc}}^{\mathrm{qpc}}/\sqrt{2}$ at saturation [16,22]. Surprisingly, we find T_{exc} at long L saturates about $\approx 13\%$ below this lower bound [displayed as a dotted line in Fig. 2(b)]. Such a discrepancy is significantly

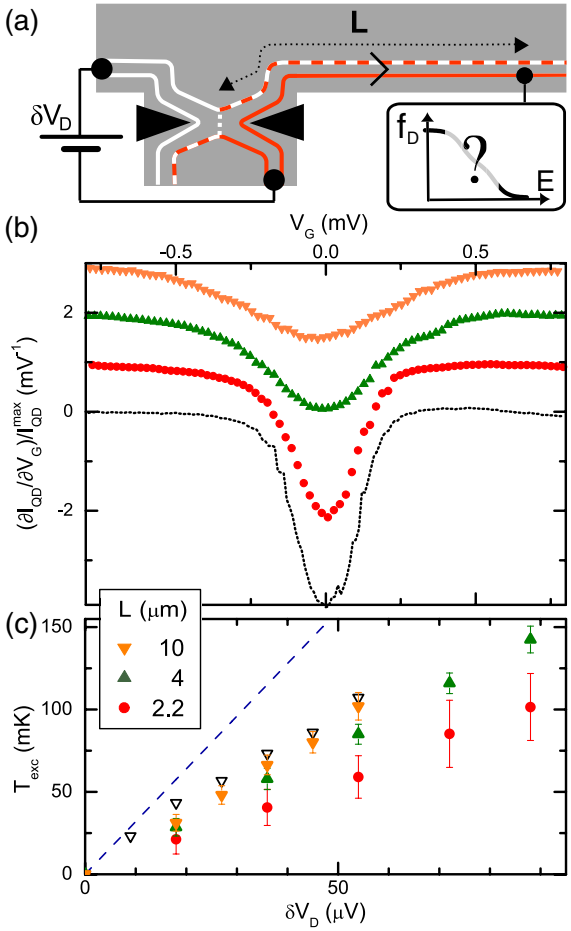

FIG. 3 (color online). (a) The inner EC is driven out of equilibrium. (b) Raw data at $\delta V_D = 0$ (dotted line) and $\delta V_D = 54$ μV (symbols), shifted vertically for several L. The dip broadens as L is increased. (c) Excess temperatures extracted from the data (full symbols) and prediction at the QPC output (dashed line). The outer EC heats up as L is increased, up to an excess temperature close to that when driving the outer EC out of equilibrium [$T_{\mathrm{exc}}(L = 10$ μm) in Fig. 2(c) are shown here as open symbols ($\bigtriangledown$)].

larger than experimental error bars. Although a good agreement data theory was reached in [22] assuming *ad hoc* the presence of a hidden third EC, one may wonder if the discrepancy results from the perturbative treatment of interactions. Note that the weak interaction hypothesis could not be checked in [22], due to the unknown length scaling factor in the theory.

Alternatively, density-density interactions between copropagating 1DCFs can be handled nonperturbatively using the bosonization technique [23]. Within this framework, edge states are depicted as collective magnetoplasmon modes. For strong enough interactions, these are fully delocalized over the ECs [12,24]. At filling factor 2, where the two ECs have opposite spin polarities, this yields spinless charge waves and chargeless spin waves propagating at different velocities. These edge states appear strikingly different from quasiparticles, where both charge and spin propagate at the same speed. Motivated by the present experiment, $T_{\rm exc}$ was recently calculated in the bosonization framework [25]. Assuming strong interactions and a standard drift velocity 10^5 m/s, calculations are found to reproduce the measured nonlinear shape of $T_{\rm exc}(\delta V_D)$ and also the energy relaxation length scale, without the need to introduce disorder [25]. However, the same lower bound $T_{\rm exc}^{\rm qpc}/\sqrt{2}$ was confirmed for arbitrary interaction strength between two 1DCF branches. In [25], the data are reproduced quantitatively by assuming *ad hoc* 25% of the energy leaks out toward other degrees of freedom.

The main outcome of the data-theory comparisons is that additional states need to be taken into account. Experimental observations, in particular, the saturation at the same hot Fermi distribution for both $L = 10$ and 30 μm, put stringent constraints on these states. The predicted internal EC modes mentioned in scenario (iii) seem plausible candidates. However, additional experiments not shown here demonstrate that 1DCFs and internal modes localized in the same outer EC do not exchange energy [20]. Although this weakens the internal modes hypothesis, note that energy exchanges with the inner EC's internal modes were not dismissed.

One conceptually important question concerns the nature of the pertinent edge excitations. Are these better described as Fermi quasiparticles localized in an EC or as delocalized bosonic collective states? The above comparison with theories did not permit discrimination. Nevertheless, the experimental results can be used to test whether the quasiparticle description is self-consistent. Indeed, a lower bound for the 1DCF's lifetime can be obtained from $L_{\rm inel}$, by using the range of drift velocities $v_D \in [0.5, 5] \times 10^5$ m/s measured in similar structures at $\nu_L = 2$ [16,26]. Applying the time-energy uncertainty relation, one finds for $\delta V_D = 36$ μV that the energy linewidth of 1DCF states $\Delta E > \hbar v_D/2L_{\rm inel} \in [6, 70]$ μeV is of the same order or larger than their characteristic energy $k_B T_{\rm exc}^{\rm qpc}(\delta V_D = 36\ \mu{\rm V}) \approx 10$ μeV, and therefore are ill-defined electronic edge excitations. Consequently, although the 1DCF representation of edge states is very powerful at short distances, the observed short $L_{\rm inel}$ challenges the description of quantum Hall excitations as quasiparticles localized in one edge channel.

The authors gratefully acknowledge discussions with A. Anthore, M. Büttiker, P. Degiovanni, C. Glattli, P. Joyez, I. Neder, F. Portier, H. Pothier, P. Roche, and E. Sukhorukov. This work was supported by the ANR (ANR-05-NANO-028-03).

*Corresponding author.
frederic.pierre@lpn.cnrs.fr

[1] B. I. Halperin, Phys. Rev. B **25**, 2185 (1982); M. Büttiker, *ibid.* **38**, 9375 (1988).
[2] Y. Ji *et al.*, Nature (London) **422**, 415 (2003).
[3] P. Samuelsson, E. V. Sukhorukov, and M. Büttiker, Phys. Rev. Lett. **92**, 026805 (2004).
[4] S. Ol'khovskaya *et al.*, Phys. Rev. Lett. **101**, 166802 (2008).
[5] I. Neder *et al.*, Nature (London) **448**, 333 (2007).
[6] R. Ionicioiu, G. Amaratunga, and F. Udrea, Int. J. Mod. Phys. B **15**, 125 (2001); T. M. Stace, C. H. W. Barnes, and G. J. Milburn, Phys. Rev. Lett. **93**, 126804 (2004).
[7] E. Bieri *et al.*, Phys. Rev. B **79**, 245324 (2009).
[8] I. Neder *et al.*, Nature Phys. **3**, 534 (2007).
[9] L. V. Litvin *et al.*, Phys. Rev. B **75**, 033315 (2007).
[10] P. Roulleau *et al.*, Phys. Rev. Lett. **100**, 126802 (2008).
[11] G. Seelig and M. Büttiker, Phys. Rev. B **64**, 245313 (2001); J. T. Chalker, Y. Gefen, and M. Y. Veillette, *ibid.* **76**, 085320 (2007); E. V. Sukhorukov and V. V. Cheianov, Phys. Rev. Lett. **99**, 156801 (2007); S.-C. Youn, H.-W. Lee, and H.-S. Sim, *ibid.* **100**, 196807 (2008); P. Degiovanni, Ch. Grenier, and G. Fève, Phys. Rev. B **80**, 241307(R) (2009).
[12] I. P. Levkivskyi and E. V. Sukhorukov, Phys. Rev. B **78**, 045322 (2008).
[13] H. Pothier *et al.*, Phys. Rev. Lett. **79**, 3490 (1997).
[14] Y.-F. Chen *et al.*, Phys. Rev. Lett. **102**, 036804 (2009).
[15] C. Altimiras *et al.*, Nature Phys. **6**, 34 (2010).
[16] See supplementary material at http://link.aps.org/supplemental/10.1103/PhysRevLett.105.056803 for additional experimental details, data, and analysis.
[17] B. J. van Wees *et al.*, Phys. Rev. Lett. **62**, 1181 (1989).
[18] I. L. Aleiner and L. I. Glazman, Phys. Rev. Lett. **72**, 2935 (1994); C. de C. Chamon and X. G. Wen, Phys. Rev. B **49**, 8227 (1994).
[19] D. B. Chklovskii, B. I. Shklovskii, and L. I. Glazman, Phys. Rev. B **46**, 4026 (1992); A. H. MacDonald, S. R. E. Yang, and M. D. Johnson, Aust. J. Phys. **46**, 345 (1993).
[20] C. Altimiras *et al.*, arXiv:1007.0974.
[21] P. Roulleau *et al.*, Phys. Rev. Lett. **101**, 186803 (2008).
[22] A. M. Lunde, S. E. Nigg, and M. Büttiker, Phys. Rev. B **81**, 041311(R) (2010).
[23] T. Giamarchi, *Quantum Physics in One Dimension* (Oxford University Press, USA, 2003).
[24] X. G. Wen, Phys. Rev. Lett. **64**, 2206 (1990).
[25] P. Degiovanni *et al.*, Phys. Rev. B **81**, 121302(R) (2010).
[26] H. Kamata *et al.*, Phys. Rev. B **81**, 085329 (2010).